ผลของสปีชีส์เหล็กบน Fe-MCM-41 ต่อประสิทธิภาพการเร่งปฏิกิริยาฟีนอลไฮดรอกซิเลชัน

Effects of Iron Species on Catalytic Performance for Phenol Hydroxylation of Fe-MCM-41

Waenkaew Pantupho[1], Krittanun Deekamwong[2], Sanchai Prayoonpokarach[2], Jatuporn Wittayakun[2], Sirinuch Loiha[1*]

[1]Materials Chemistry Research Center, Department of Chemistry, Faculty of Science, Khon Kaen University, Khon Kaen 40002, Thailand

[2]School of Chemistry, Institute of Science, Suranaree University of Technology, Nakhon Ratchasima 30000, Thailand

*Corresponding Author, E-mail: sirilo@kku.ac.th

บทคัดย่อ

ตัวเร่งปฏิกิริยาเหล็กบนตัวรองรับ HMCM-41 ที่มีปริมาณเหล็กร้อยละ 5 โดยน้ำหนัก สังเคราะห์ขึ้นจากวิธีการเอิบชุ่ม (5Fe/HZSM-5_IMP) และวิธีไฮโดรเทอร์มอล (5Fe/HZSM-5_HYD) มีโครงสร้างเป็นเฮกซะโกนอลที่มีความเป็นผลึกสูง สปีชีส์ของเหล็กที่กระจายตัวบนตัวเร่งปฏิกิริยาที่สังเคราะห์จากวิธีเอิบชุ่ม มีโครงสร้างผลึกแบบแมกนีไทท์หรืออินเวอร์สสปีเนล ของ Fe_3O_4 สำหรับตัวเร่งปฏิกิริยาที่สังเคราะห์ขึ้นแบบไฮโดรเทอร์มอล พบโครงสร้างเหล็กแบบเททระฮีดรอนแทนที่ในเฟรมเวอร์ค MCM-41 ผลการทดสอบการเร่งปฏิกิริยาฟีนอลไฮดรอกซิเลชันของตัวเร่งปฏิกิริยาทั้งสองชนิด พบว่า 5Fe/HZSM-5_HYD มีความสามารถในการเร่งปฏิกิริยาที่สูงกว่า 5Fe/HZSM-5_IMP สัดส่วนการคัดเลือกผลิตภัณฑ์แคทิคอล/ไฮโดรควิโนน เป็น 70/30 และ 60/40 สำหรับ 5Fe/HZSM-5_IMP และ 5Fe/HZSM-5_HYD ตามลำดับ 5Fe/HZSM-5_HYD มีความจำเพาะต่อไฮโดรควิโนนเพิ่มขึ้นเมื่อเปรียบเทียบกับ 5Fe/HZSM-5_IMP เป็นผลมาจากมีสมบัติชอบน้ำต่ำของโครงสร้างเหล็กในเฟรมเวอร์ค MCM-41 ปฏิกิริยาของ 5Fe/HZSM-5_IMP มีร้อยละการคัดเลือกต่อแคทิคอลที่สูงและมีร้อยละการสูญเสียมวลเพิ่มขึ้น เนื่องจาก Fe_3O_4 มีสมบัติชอบน้ำที่สูงจึงเกิดการดูดซับที่แข็งแรงของสารตั้งต้น ซึ่งมีแนวโน้มการเสื่อมสภาพเนื่องจากการสะสมของโมเลกุลคาร์บอนสูง

ABSTRACT

Catalysts with 5 wt% iron supported on MCM-41 were prepared by impregnation (5Fe-MCM-41_IMP) and mixed gel hydrothermal synthesis (5Fe-MCM-41_HYD). Both catalysts showed high crystallinity of regular hexagonal structure of MCM-41. Iron species in 5Fe-MCM-41_IMP were the magnetite or inverse spinel Fe_3O_4 whereas that in 5Fe-MCM-41_HYD was tetrahedral Fe(III) in the MCM-41 framework. Catalytic activity and selectivity for phenol hydroxylation of the catalysts were determined. A higher catalytic activity of 5Fe-MCM-41_HYD over 5Fe-MCM-41_IMP was observed. Catalytic selectivities in term of catechol to hydroquinone ratio were 70:30 and 60:40 for 5Fe-MCM-41_IMP and 5Fe-MCM-41_HYD, respectively. The selectivity to hydroquinone was improved by the presence of tetrahedral Fe(III) in the MCM-41 framework due to its low hydrophilicity. The Fe_3O_4 species on 5Fe-MCM-41_IMP was more selective to catechol and favorable for strong adsorption of phenol due to its high hydrophilicity leading to catalytic deactivation by carbon deposition.

คำสำคัญ: Fe-MCM-41 ปฏิกิริยาฟีนอลไฮดรอกซิเลชัน Fe_3O_4 แคทีคอล ไฮโดรควิโนน

Keywords: Fe-MCM-41, Phenol hydroxylation, Fe_3O_4, Catechol, Hydroquinone

1. INTRODUCTION

Catechol (CAT) and hydroquinone (HQ) are dihydroxylbenzenes which can be synthesized by direct phenol hydroxylation using a clean oxidant like H_2O_2 as shown in scheme 1. Benzoquinone (BQ) is formed as a minor product of the reaction.

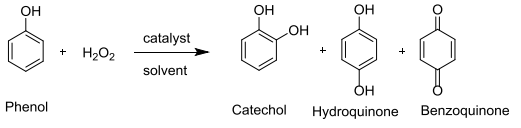

Scheme 1 Phenol hydroxylation reaction.

CAT and HQ have been widely used as antioxidants in industrial synthesis, polymerization inhibitors, photography chemicals and intermediates in fine chemical industries (Preethi et al., 2008). Porous crystalline catalysts such as microporous titanium silicalites (TS) (Zhang et al., 2010), zeolites (Mohameda et al., 2003) and mesoporous silicates (Subrahmanyam et al., 2008; Choi et al., 2006; Lee et al., 2001; Nesterenko et al., 2003; Chumee et al., 2009) have been reported to be active for phenol hydroxylation. The mesoporous silicate materials such as MCM-41 and MCM-48 exhibited a catalytic potential for liquid phase reactions due to their high surface area, large pore volume, regular structure, uniform pore size distribution and high thermal stability (Subrahmanyam et al., 2008).

Transition metals with redox property such as Mn, Cu and Fe are introduced into the

porous materials as active sites for selective oxidation. Mesoporous silicate containing iron (Fe) showed a better performance in phenol hydroxylation than other transition metals. (Preethi et al., 2008; Zhang et al., 2010; Lee et al., 2001; Nesterenko et al., 2003; Szegedi et al., 2004).

Phenol hydroxylation using Fe-based catalysts has been known to proceed via a redox mechanism involving Fe(II)/Fe(III) redox pair (Choi et al., 2006). Hydroxyl radical (•OH) and superoxide radical (•OOH) are primarily created by reaction of H_2O_2 with Fe(II) and Fe(III) as shown in scheme 2 (Yang et al., 2005). The Fe(II) species is more favorable for the formation of •OH than the Fe(III) species.

$$Fe^{2+} + H_2O_2 \rightarrow Fe^{3+} + H_2O + \dot{O}H \quad (k1 = 58\ mol^{-1}dm^3s^{-1}) \qquad (1)$$

$$Fe^{3+} + H_2O_2 \rightarrow Fe^{2+} + H_2O + \dot{O}OH \quad (k2 = 0.02\ mol^{-1}dm^3s^{-1}) \qquad (2)$$

Scheme 2 Redox mechanism of Fe^{n+} with H_2O_2

It has been shown that the catalytic performance of mesoporous catalysts containing Fe catalysts depends on Fe active species, strongly resulting from preparation methods (Song et al., 2010). For hydroxylation reaction, the catalytic activity and selectivity mainly depend on dispersion of iron inside and outside the framework of mesoporous supports (Zhang et al., 2010).

Iron oxide nanoparticles of Fe_2O_3 with Fe in octahedral coordination (Subrahmanyam et al., 2008) and magnetite (Fe_3O_4) with Fe in tetrahedral and octahedral coordination (Song et al., 2010; Zhong et al., 2007) can be produced by impregnation method. The Fe(III) in the framework of mesoporous silicate with tetrahedral coordination could be produced by hydrothermal synthesis (Choi et al., 2006). The iron oxide nanoparticles by impregnation could promote better redox reactions (scheme 2) than the tetrahedral Fe in the mesoporous framework by hydrothermal method (Preethi et al., 2008). Iron oxide particles were suggested as active species for phenol hydroxylation. However, the presence of octahedral Fe sites in iron oxide particles also influenced the catalytic activity (Choi et al., 2006). Octahedral Fe species showed lower catalytic activity than tetrahedral Fe in mesoporous framework. Therefore, effects of iron active species on MCM-41 containing octahedral and tetrahedral sites for phenol hydroxylation have been investigated in this work.

For iron oxide particles, Fe_2O_3 was reported to give a poorer conversion and selectivity in aromatic hydroxylation than Fe_3O_4 species (Song et al., 2010; Zhong et al., 2010). The reason is that the oxidant H_2O_2 tends to decompose directly to H_2O and O_2 over strong acid sites of Fe_2O_3, only some molecules of H_2O_2 take part in the catalytic reaction. The highly active species of Fe_3O_4 for

hydroxylation is promoted by the spontaneous reduction of Fe(III) on the defect sites of the mesoporous support (Song et al., 2010).

In this work, different iron active species on MCM-41 (Fe-MCM-41) were synthesized using impregnation and hydrothermal methods. Effects of the iron active species on catalytic activity and selectivity for phenol hydroxylation were determined.

2. MATERIALS AND METHODS

2.1 Materials

Rice husk silica (SiO_2) and ferric nitrate ($Fe(NO_3)_3 \cdot 9H_2O$, Merck, 98.5 wt%) were used as the precursors of silicon and iron, respectively. The cationic surfactant cetyltrimethylammonium bromide (CTABr, Fluka, 98%) was used as a template. The solutions of sodium hydroxide (RCI Labscan) and sulfuric acid (Carlo-Erba) were used to adjust the pH of the MCM-41 gels. Phenol (Panreac, 99%) and H_2O_2 (Merck, 30 wt%) were used as the starting materials for catalytic activity test.

2.2 Synthesis of 5Fe-MCM-41_IMP

The MCM-41 was synthesized by hydrothermal method (HYD) using rice husk silica source as reported by Chumee et al. (2009). The siliceous gel was prepared by dissolving 2.0 g rice husk silica powder in NaOH solution. The mixture was stirred until a clear solution was obtained. CTABr template was dissolved in 15 mL DI water then slowly added to the siliceous solution with stirring provided for 30 min. For gelation step, the pH of the mixed solution was adjusted to 11 by 2 M H_2SO_4. The prepared gel was then transferred to a Teflon-lined autoclave for crystallization at 110 ºC for 48 h. The solid was separated from the solution by filtration, washed, dried and calcined at 500 ºC for 6 h. White powder of MCM-41 was obtained.

The post-synthesis of Fe-contained MCM-41 catalyst was done by impregnation method (IMP). $Fe(NO_3)_3 \cdot 9H_2O$ (0.61 g) was dissolved in 1.0 mL DI water and slowly dropped to 1.0 g of calcined MCM-41. The impregnated sample was dried at 60 ºC for 24 h and calcined at 500 ºC for 6 h to give 5Fe-MCM-41_IMP.

2.3 Preparation of 5Fe-MCM-41_HYD

The 5 wt% Fe containing MCM-41 was synthesized using the same procedure as that for MCM-41. $Fe(NO_3)_3 \cdot 9H_2O$ (0.61 g) was dissolved in DI water and added dropwise to the mixture of siliceous solution and template. The mixture was crystallized in a Teflon line autoclave at 110 ºC for 48 h. The crystalline 5Fe-MCM-41_HYD was separated from the solution by filtration, washed, dried and calcined at 500 ºC for 6 h.

2.4 Catalytic testing

Phenol hydroxylation was carried out under a reflux condition in a 250 mL three-

necked round bottom flask. Phenol (2.11 g) was added to 25 mL DI water. A 0.05 g catalyst was added to the phenol solution then stirred for 30 min. Hydrogen peroxide (30 wt%) was added dropwise through a septum to the mixture to give H_2O_2:phenol molar ratio of 1:1. The reaction temperature was 70 ºC. The reaction mixtures were collected every 10 min from 10 to 30 min. The collection was then in every 60 min from 60 to 300 min. All the collected samples were analyzed by a gas chromatograph (Shimadzu) equipped with DB-5 coated capillary column and flame ionization detector. Catalytic conversion, activity, selectivity and mass loss were calculated as follow;

$$\text{Conversion (\%)} = \frac{\text{(mole of phenol input - mole of phenol output)}}{\text{mole of phenol input}} \times 100$$

$$\text{Activity (\%)} = \frac{\text{Conversion amount of phenol}}{\text{mass of Fe in catalyst}} \times 100$$

$$\text{Selectivity to CAT (\%)} = \frac{\text{mole of CAT}}{\text{(mole of CAT +mol of HQ + mole of BQ)}} \times 100$$

$$\text{Mass loss (\%)} = \frac{\text{(mole of carbon input – mole of carbon output)}}{\text{mole of carbon input}} \times 100$$

2.5 Characterization of the catalysts

Phase of the catalyst was studied by powder X-ray diffractometer (XRD), Bruker D8 ADVANCE, using Cu K_α radiation. The morphology of the catalyst was examined by transmission electron microscope (TEM), TECNAI G2 20. Elemental compositions of the catalysts were analyzed by wavelength dispersive X-ray Fluorescence (WDXRF), PaNalytical, Axios-Max, with Si(PIN) detector. Specific BET surface area and pore volume of the catalysts were determined by N_2-adsorption desorption technique, Quanta chrome instrument (Autosorb-1 series). The iron species on the catalysts were determined using UV-Vis diffuse reflectance spectroscopy and X-ray absorption spectroscopy (XAS) technique at synchrotron light research institute (public organization), SLRI.

3. RESULTS AND DISCUSSION

3.1 Characterization of 5Fe-MCM-41_IMP and 5Fe-MCM-41_HYD

XRD patterns in Figure 1 indicated characteristic peaks of (100), (110) and (200) planes in the 2θ ranges of 2-5º corresponded to a regular hexagonal channel of MCM-41 (Choi et al., 2006). The mesoporous structure was well observed even after addition of Fe by HYD and IMP methods. The lattice spacing (d-spacing) of hexagonal arrays on the catalysts was calculated from (100) plane as shown in Table 1. The d-spacing value observed from 5Fe-MCM-41_HYD was slightly higher than that from 5Fe-MCM-41_IMP. This result suggested the incorporation of iron species inside the framework of MCM-41. The reason was that the ionic radius of Fe(III) (0.064 nm) was larger than the radius of Si (IV) (0.026 nm) (Preethi et al., 2008). The lattice contraction of 5Fe-MCM-41_IMP was probably

due to the increase of the degree of connectivity within the silica walls of MCM-41 (Fröba et al., 1999). Peaks corresponded to iron oxide particles were not observed which suggested high dispersion of Fe species on both 5Fe-MCM-41_HYD and 5Fe-MCM-41_IMP (Subrahmanyam et al., 2008).

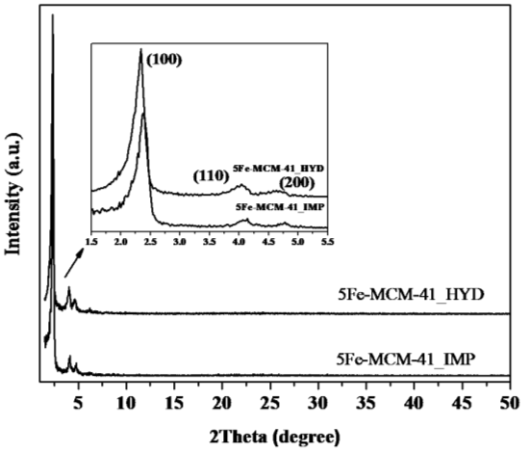

Figure 1 XRD patterns of 5Fe-MCM-41_HYD and 5Fe-MCM-41_HYD

TEM images of MCM-41, 5Fe-MCM-41_HYD and 5Fe-MCM-41_IMP are shown in Figure 2. Uniform channels with hexagonal arrays with lattice spacing about 2.5 nm were clearly observed on MCM-41 (Figure 2a and 2b). Short-ranged order and larger lattice spacing of the hexagonal arrays were observed on 5Fe-MCM-41_HYD and 5Fe-MCM-41_IMP (Figure 2c and 2d) consistent with the XRD results. Amorphous silicate was observed more clearly on 5Fe-MCM-41_IMP as shown in Figure 2d.

Elemental analyses on both of catalysts are shown in Table 1. The Fe content in 5Fe/MCM-41_IMP was higher than that in 5FeMCM-41_HYD. BET surface area of 5Fe-MCM-41_HYD and 5Fe-MCM-41_IMP were 1180 and 903 m^2/g, respectively. On 5Fe-MCM-41_IMP which was prepared by impregnation, particles of iron oxides resided on the surface and resulted in lower surface area. In addition, the lower surface area could indicate partial pore blocking.

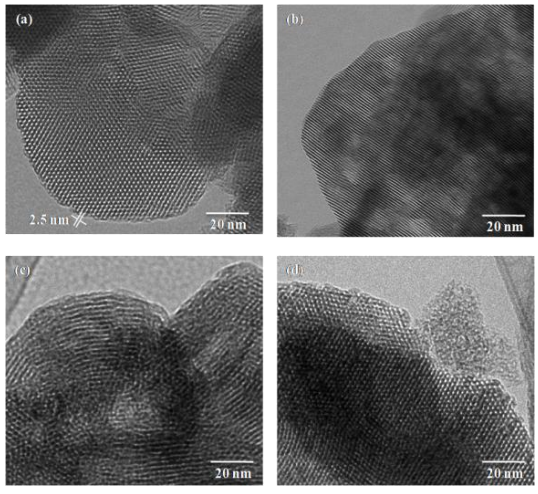

Figure 2 TEM images of hexagonal array arrangement of MCM-41 (a) and long-range order structure MCM-41 (b) 5Fe-MCM-41_HYD (c) and 5Fe-MCM-41_IMP (d)

Table 1 2Theta and d-spacing and elemental compositions of 5Fe-MCM-41_HYD and 5Fe-MCM-4_IMP

Sample	$2\theta_{(100)}$	$d_{(100)}$ (nm)	Elemental composition		BET surface area (m^2/g)
			Si	Fe	
5Fe-MCM-41_HYD	2.34	3.77	43.8	2.9	1180
5Fe-MCM-41_IMP	2.38	3.70	43.5	3.9	903

3.2 Iron species on 5Fe-MCM-41_IMP and 5Fe-MCM-41_HYD

The XANES spectra of the catalysts at Fe K-edge compared with Fe_2O_3 and Fe_3O_4 standards are shown in Figure 3. The edge energy from 5Fe-MCM-41_HYD and 5Fe-MCM-41_IMP were similar to that of Fe(III) species. The pre-edge (Figure 3 inset) and XANES feature of 5Fe-MCM-41_IMP were more comparable to that of the Fe(II) and Fe(III) species in magnetite or inverse spinel Fe_3O_4 (Li et al., 2012; Menarda et al., 2013). The pre-edge feature of 5Fe-HMCM-41_HYD was intense and narrow suggesting the presence of tetrahedral Fe(III) species (Menarda et al., 2013).

The k^3-weight scattering functions and Fourier transforms of EXAFS spectra are shown in Figure 4. The EXAFS fitted parameters of number of neighboring atom (N), bond distance (R) and Debye-Waller factor (σ^2) are shown in Table 2. The first shell corresponded to four-coordinated Fe-O with average bond distances of 1.95 and 1.92 Å for 5Fe-MCM-41_IMP and 5Fe-MCM-41_HYD, respectively. Six-coordinated Fe-O bonds with average distance of 2.88 Å were observed only on 5Fe-MCM-41_IMP. The presence of both four-and six-coordinated Fe-O bonds on 5Fe-MCM-41_IMP indicated the magnetite species of Fe_3O_4 containing tetrahedral Fe(III), octahedral Fe(III) and tetrahedral Fe(II) (Li et al., 2012; Jiao et al., 2006). Four-coordinated Fe-O was the only species observed on 5Fe-MCM-41_HYD indicating the presence of tetrahedral Fe(III) inside MCM-41 framework (Choi et al., 2006). The second shell in the range of 2.00-3.00 Å observed from both 5Fe-MCM-41_IMP and 5Fe-MCM-41_HYD corresponded to combination of Fe-Fe and Fe-O bonds. The bond distances on both catalysts were nearly the same.

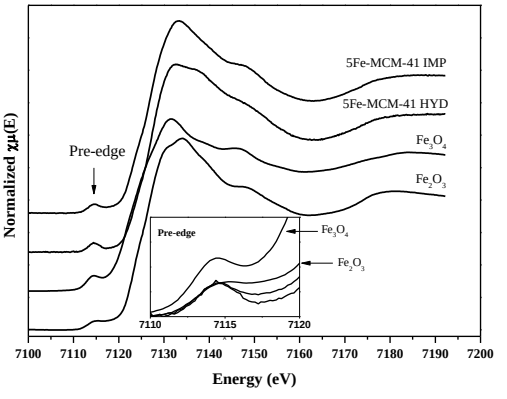

Figure 3 The normalized XANES spectra of 5Fe_MCM-41_IMP and 5Fe_MCM-41_HYD with Fe_2O_3 and Fe_3O_4 standards

However, the numbers of neighboring atoms of Fe observed on 5Fe-MCM-41_HYD was lower than that of 5Fe-MCM-41_IMP indicating a good dispersion of the Fe species on 5Fe-MCM-41_HYD (Menarda et al., 2013).

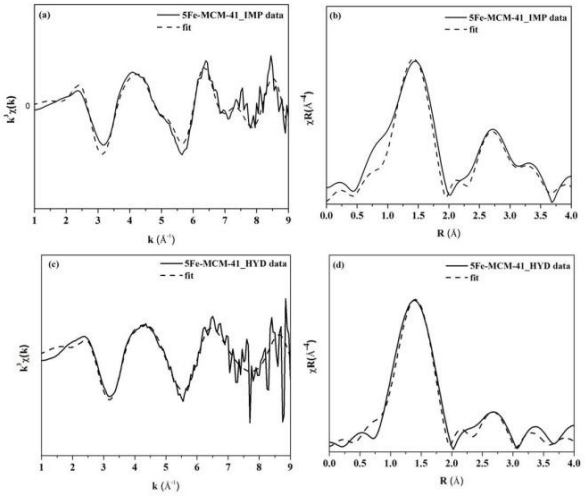

Figure 4 The k^3-weight scattering functions 5Fe-MCM-41_IMP (a) and 5Fe-MCM-41_HYD (c) and the Fourier transforms of k^3-weight EXAFS spectra of 5Fe-MCM-41_IMP (b) and 5Fe-MCM-41_HYD (d)

UV-Vis diffuse reflectance spectra in the wavelength range of 200-800 nm of 5Fe-MCM-41_IMP and 5Fe-MCM-41_HYD are shown in Figure 5. The strong absorption bands in the range of 200-320 nm with the maxima wavelength at ca. 275 nm were assigned as the dπ-pπ charge transfer between Fe and O atoms of tetrahedral Fe (III) (Subrahmanyam et al., 2008; Choi et al., 2006; Samanta et al., 2003).

The bands in the range of 350-600 nm were dominant on 5Fe-MCM-41_IMP. These bands were assigned to agglomerated clusters or nanoparticles of Fe_3O_4 having Fe with octahedral coordination (Subrahmanyam et al., 2008; Samanta et al., 2003). These bands were less intense on 5Fe-MCM-41_HYD indicating the less aggregation of iron oxide cluster or extra-framework iron (Wang et al., 2002).

3.3 Catalytic activity for phenol hydroxylation

The phenol conversions and activities of 5Fe-MCM-41_IMP and 5Fe-MCM-41_HYD are shown in Figure 6a and 6b, respectively. At 25 min, in contrast to Preethi et al. (2008), the conversion and activity of 5Fe-MCM-41_HYD was higher but became nearly the same with the longer reaction time. A lower catalytic activity of 5Fe-MCM-41_IMP suggested that octahedral Fe species (Fe_3O_4) on 5Fe-MCM-41_IMP was less active species in comparison to tetrahedral Fe(III) inside MCM-41 framework on 5Fe-MCM-41_HYD (Choi et al., 2006). However, the Fe_3O_4 species on 5Fe-MCM-41_IMP had higher activity for phenol

hydroxylation with the same reaction condition in comparison to other active species of FeO_x/MCM-41 prepared by impregnation and Fe_2O_3 nanoparticles reported in literature (Choi et al., 2006). The reason was that Fe_3O_4 species on MCM-41 could be promoted by spontaneous reduction of Fe(II)/Fe(III) in presence on H_2O_2 (scheme 2) on the defect sites of MCM-41 (Song et al., 2010).

Table 2 Fit results from EXAFS spectra of 5Fe-MCM-41_IMP and 5Fe-MCM-41_HYD

Sample/component	R (Å)	N	σ^2
5Fe_MCM-41_IMP			
Fe-O	1.95	4	0.011
Fe-O	2.88	6	0.011
Fe-Fe	3.51	12	0.015
Fe-O	3.68	12	0.007
5Fe_MCM-41_HYD			
Fe-O	1.92	4	0.010
Fe-Fe	3.50	6	0.013
Fe-O	3.67	6	0.001

Mass loss percentage indicated formation of undesired products from phenol hydroxylation. The mass loss percentage of 5Fe-MCM-41_HYD was lower than that of 5Fe-MCM-41_IMP. This results indicated that the catalyst of 5Fe-MCM-41_HYD which contained tetrahedral Fe(III) in MCM-41 framework was more selective to phenol hydroxylation products.

The catalytic selectivity to CAT, HQ and BQ of 5Fe-MCM-41_IMP and 5Fe-MCM-41_HYD are shown in Figure 7. Both catalysts were more selective to CAT than HQ and BQ products. The selectivity in term of CAT:HQ from 5Fe-MCM-41_IMP and 5Fe-MCM-41_HYD were approximately 70:30 and 60:40, respectively. These results suggested that the Fe in magnetite Fe_3O_4 species of 5Fe-MCM-41_IMP was more selective to CAT. The selectivity to HQ was improved by the 5Fe-MCM-41_HYD which contained tetrahedral Fe(III) species in the framework.

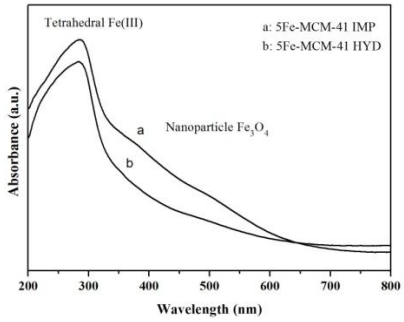

Figure 5 UV-Vis spectroscopy of 5Fe-MCM-41_IMP and 5Fe-MCM-41_HYD

The high selectivity to CAT on 5Fe-MCM-41_IMP was explained by high hydrophilicity of Fe_3O_4 particles as well as Fe_2O_3 particles reported by Choi et al. (2006). Thermodynamically more favored CAT formation was possible when both phenol and H_2O_2 adsorbed on the same active site of Fe_3O_4 particles. The hydrophilic sites of Fe_3O_4 favored chemisorption of H_2O_2 and phenol. However, the strong adsorption on the hydrophilic sites could lead to undesired reactions like formation of tarry products and BQ (Preethi et al., 2008; Choi et al., 2006).

The HQ selectivity on phenol hydroxylation was improved by the 5Fe-MCM-41_HYD catalysts. This was due to the low redox potential of substituted tetrahedral Fe(III) in MCM-41 framework species on 5Fe-MCM-41_HYD (Preethi et al., 2008; Choi et al., 2006). This species preferred adsorption of H_2O_2 leaving more phenol in the un-adsorbed state which was a requirement for selective HQ (Preethi et al., 2008).

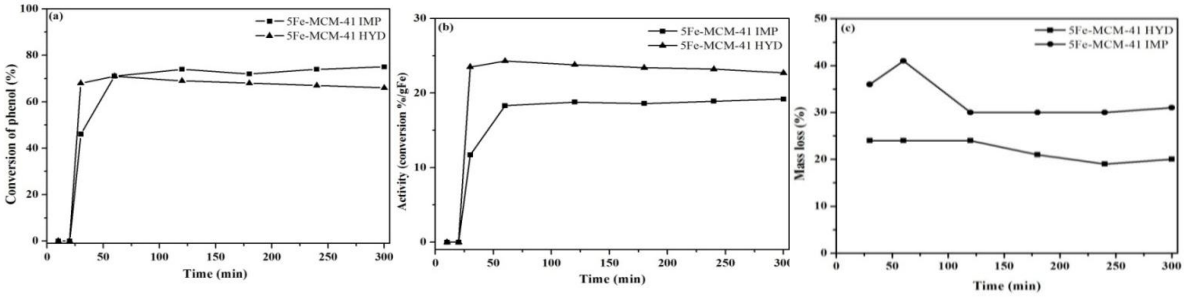

Figure 6 Conversion (a) activity (b) mass loss (c) for phenol hydroxylation of 5Fe-MCM-41_IMP and 5Fe-MCM-41_HYD catalysts

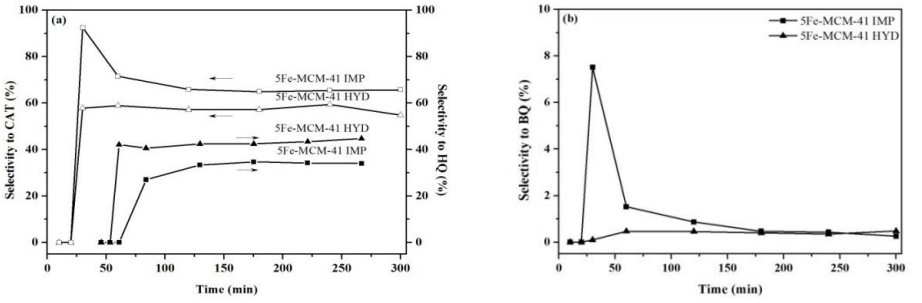

Figure 7 Selectivity to CAT and HQ (a) and BQ (b) for phenol hydroxylation of 5Fe-MCM-41_IMP and 5Fe-MCM-41_HYD

4. CONCLUSION

5Fe-MCM-41_IMP and 5Fe-MCM-41_HYD were prepared by impregnation and hydrothermal method, respectively. Hexagonal structures of MCM-41 were obtained on both of catalysts. Iron species on 5Fe-MCM-41_IMP and 5Fe-MCM-41_HYD were the magnetite or inverse spinel Fe_3O_4 and substituted tetrahedral Fe(III) inside MCM-41 framework, respectively. 5Fe-MCM-41_HYD showed higher catalytic activity for phenol hydroxylation than that of 5Fe-MCM-41_IMP. Moreover, the 5Fe-MCM-41_HYD could improve the catalytic selectivity to HQ. These results indicated that tetrahedral Fe(III) inside MCM-41 framework was higher active to phenol hydroxylation than Fe_3O_4. The reason could be explained by their hydrophilicity. Due to high hydrophilicity of Fe_3O_4, high mass loss percentage of reaction was observed by 5Fe-MCM-41_IMP.

5. ACKNOWLEDGEMENTS

The authors appreciated the financial supports from the Thailand Research Fund (TRF MRG5480049), the Center of Excellence for Innovation in Chemistry (PERCH-CIC) and Research Support Scholarship, Khon Kaen University.

6. REFERENCES

Choi, J. S., Yoon, S. S., Jang, S. H.,W. S. (2006). Phenol hydroxylation using Fe-MCM-41 catalysts. Catalysis Today 111(3-4): 280-287.

Chumee, J., Grisdanurak, N., Neramittagapong, A., Wittayakun, J. (2009). Characterization of platinum–iron catalysts supported on MCM-41 synthesized with rice husk silica and their performance for phenol hydroxylation. Science and Technology of Advanced Materials.10: 015006.

Fröba, M., Köhn, R., Bouffau, G. (1999). Fe_2O_3 Nanoparticles within mesoporous MCM-48 silica: In situ formation and characterization. Chemistry of matarials 11(10): 2858-2865.

Jiao, F., Jumas, J. C., Womes, M., Chadwick, A. V., Harrison,A., Bruce, P. G. (2006). Synthesis of ordered mesoporous Fe_3O_4 and γ-Fe_2O_3

with crystalline walls using post-template reduction/oxidation. Journal of American Chemical Society 128(39): 12905-12909.

Lee, C. W., Ahn, D. H., Wang, B, Hwang, J. S., Park,S. E. (2001). Hydroxylation of phenol over surface functionalized MCM-41 supported metal catalyst. Microporous and Mesoporous Materials 44-45: 587-594.

Li, B., Xu, J., Li, X., Liu, J., Zuo, S., Pan, Z., WuZ. (2012). Bimetallic iron and cobalt incorporated MFI/MCM-41 composite and its catalytic properties. Materials Research Bulletin 47(5): 1142-1148.

Menarda, M. C., Marschilok,A. C., Takeuchi, K. J., Takeuchi, E. S. (2013). Variation in the iron oxidation states of magnetite nanocrystals as a function of crystallite size: The impact on electrochemical capacity. Electrochimica Acta 94(1): 320-326.

Mohameda, M. M., Eissa, N.A. (2003). Characterization of intrazeolitic Fe^{3+} prepared by chemical vapor deposition of $[(C_5H_5)Fe(CO)_2]_2$ inside NaY andFSM-16 zeolites and their catalytic activities towards phenol hydroxylation. Materials Research Bulletin 38(15): 1993-2007.

Nesterenko, N.S., Ponomoreva, O.A.,Yuschenko, V.V., Ivanova, I.I., Testa, F., Di Renzo, F., Fajula, F. (2003). Dehydrogenation of ethylbenzene and isobutane over Ga- and Fe-containing mesoporous silicas. Applied Catalysis A: General 254(2): 261–272.

Preethi, M. E.L., Revathi, S., Sivakumar, T., Manikandan, D., Divakar, D. Rupa, A. V., Palanichami, M. (2008). Phenol hydroxylation using Fe/Al-MCM-41 catalysts. Catalysis Letters 120(1): 56–64.

Samanta, S., Giri, S., Sastry, P. U., Mal, N. K., Manna, A., Bhaumik. A., (2003). Synthesis and characterization of iron-rich highly ordered mesoporous Fe-MCM-41. Industrial Engineering and Chemistry Research 42(13): 3012-3018.

Song, S., Yang, H., Rao, R., Liu, H., Zhang, A. (2010). High catalytic activity and selectivity for hydroxylation of benzene to phenol over multi-walled carbon nanotubes supported Fe_3O_4 catalyst. Applied Catalysis A: General 375(2): 265-271.

Souzaa, W. F. D., Guimarães, I. R., Oliveira,L. C.A., Guerreiro, M. C., Guarieiro, A. L.N., Carvalho, K. T.G. (2007). Natural and H2-reduced limonite for organic oxidation by a Fenton-like system: Mechanism study via ESI-MS and theoretical calculations. Journal of Molecular Catalysis A: Chemical 278(1-2): 145-151.

Subrahmanyam, C., Viswanathan, B., Varadarajan, T.K. (2008). Synthesis, characterization and catalytic activity of mesoporous trivalent iron substituted alumino phosphates. Journal of Molecular Catalysis A: Chemical 223(1-2): 149-153.

Szegedi, Á., Kónya, Z., Méhn, D., Solymár, E., Borbély, G. P., Horváth, Z. E., Biró, L. P., Kiricsi, I. (2004). Spherical mesoporous MCM-41 materials containing transition metals: synthesis and characterization. Applied Catalysis A: General 272(1-2): 257-266.

Wang, Y., Zhang,Q., Shishido,T., Takehira, K., (2002). Characterizations of iron-containing MCM-41 and its catalytic properties in epoxidation of styrene with hydrogen peroxide. Journal of Catalysis 209(1): 186-196.

Yang, G. P., Zhao, X. K., Sun, X. J., Lu, X. L. (2005). Oxidative degradation of diethyl phthalate by photochemically-enhanced Fenton reaction. Journal of Hazardous Materials 126(1-3): 112–118.

Zhang, G., Long, J., Wang, X., Zhang, Z., Dai, W., Liu, P., Li, Z., Wu, L., Fu, X. (2010). Catalytic role of Cu sites of Cu/MCM-41 in phenol hydroxylation. Langmuir 26(2): 1362-1371.

Zhang, S., Zhao, X., Niu, H., Shi, Y., Cai, Y., Jiang. G. (2009). Superparamagnetic Fe_3O_4 nanoparticles as catalysts for the catalytic oxidation of phenolic and aniline compounds. Journal of Hazardous Materials 167(1-3): 560-566.

Zhong, Y., Li, G., Zhu, L., Yan, Y., Wu, G., Hu, C. (2007). Low temperature hydroxylation of benzene to phenol by hydrogen peroxide over Fe/activated carbon catalyst. Journal of Molecular Catalysis A: Chemical 272(1-2): 169-173.

❑❑❑❑❑